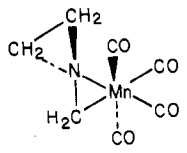

16

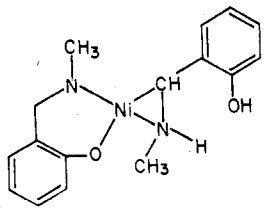

17

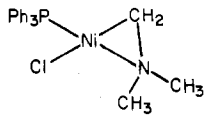

18

The structure of **6** indicates no unusual intermolecular contacts. The shortest intermolecular distances occur for O_1–H_{35} ($x, y, -1 + z$) 2.64 Å, O_1–H_{46} ($1.5 - x, -y, 0.5 + z$) 2.66 Å, O_1–H_{14} ($0.5 - x, -y, -0.5 + z$) 2.80 Å, O_2–H_9 ($0.5 - x, -y, 0.5 + z$) 2.83 Å, O_3–H_{17} ($1 - x, -0.5 + y, 1.5 - z$) 2.81 Å, and O_4–H_{15} ($1 - x, -0.5 + y, 0.5 - z$) 2.76 Å which compare with the sum of the van der Waals radii for oxygen and hydrogen of 2.6 Å.[25] These contacts are indicated in Figure 3. All intermolecular hydrogen–hydrogen distances are more than 0.20 Å greater than the value of 2.4 Å for the sum of the van der Waals radii of two hydrogen atoms.

Acknowledgment. We thank the donors of the Petroleum Research Fund, administered by the American Chemical Society, for support of this research and Professor E. K. Barefield for a preprint of the study by himself and co-workers cited in this work.[4b] Computer time was furnished by the UCLA Campus Computing Network. The authors thank Dr. B. T. Huie for help in use of the diffractometer.

Registry No. **6**, 56725-20-3.

Supplementary Material Available: Figure 4, stereoview of unit cell, and Table I, the observed and calculated structure factors (6 pages). Ordering information is given on any current masthead page.

References and Notes

(1) (a) Taken in part from the dissertation of S. A. S. Crawford, UCLA, 1975. (b) This is part 13 in a series on metalation reactions; for part 12 see S. S. Crawford and H. D. Kaesz, *Inorg. Chem.*, preceding paper in this issue.
(2) S. S. Crawford, G. Firestein, and H. D. Kaesz, *J. Organomet. Chem.*, **91**, C57 (1975).
(3) (a) E. W. Abel, R. J. Rowley, R. Mason, and K. M. Thomas, *J. Chem. Soc., Chem. Commun.*, 72 (1974); cf. E. W. Abel and R. J. Rowley, *J. Chem. Soc., Dalton Trans.*, 1096 (1975); see also (b) C. W. Fong and G. Wilkinson, *ibid.*, 1100 (1975).
(4) (a) M. Matsumoto, K. Nakatsu, K. Tani, A. Nakamura, and S. Otsuka, *J. Am. Chem. Soc.*, **96**, 6777 (1974); (b) D. J. Sepelak, C. G. Pierpont, E. K. Barefield, J. T. Budz, and C. A. Poffenberger, *ibid.*, **98**, 6178 (1976).
(5) (a) J. Chatt and J. M. Davidson, *J. Chem. Soc.*, 843 (1965); (b) F. A. Cotton, B. A. Frenz, and D. L. Hunter, *J. Chem. Soc., Chem. Commun.*, 755 (1974).
(6) (a) J. W. Rathke and E. L. Muetterties, *J. Am. Chem. Soc.*, **97**, 3272 (1975); (b) H. H. Karsch, H. F. Klein, and H. Schmidbauer, *Angew. Chem., Int. Ed. Engl.*, **14**, 637 (1975).
(7) Numbers given in parentheses throughout this paper are the estimated standard deviations and refer to the last digit given. The automatic centering, indexing, and least-squares programs of the diffractometer were used to obtain these parameters and their estimated standard deviations.
(8) (a) The programs used in this work included locally written data reduction programs; JBPATT, JBFOUR, and PEAKLIST, modified versions of Fourier programs written by J. Blount; local version of ORFLS (Busing, Martin, and Levy), structure factor calculations and full-matrix least-squares refinement; HPOSN (Hope) to calculate tentative hydrogen positions; ORTEP (Johnson) figure plotting; distances, angles, and error computations; all calculations were performed on the IBM 360-91 computer operated by the UCLA Campus Computing Network. (b) The reduction of diffractometer data is described in part 9 of this series: R. J. McKinney, C. B. Knobler, B. T. Huie, and H. D. Kaesz, *J. Am. Chem. Soc.*, **99**, 2988 (1977).
(9) Conventional R index, $R_1 = \sum||F_o| - |F_c||/\sum|F_o|$; weighted residual factor $R_2 = [\sum w(|F_o| - |F_c|)^2/\sum w|F_o|^2]^{1/2}$, where the weight $w = [1/\sigma(F_o)]^2$. The function $\sum w||F_o| - |F_c||^2$ was minimized.
(10) D. T. Cromer and D. Liberman, *J. Chem. Phys.*, **53**, 1891 (1970).
(11) H. P. Hanson, F. Herman, J. D. Lea, and S. Skillman, *Acta Crystallogr.*, **17**, 1040 (1964).
(12) R. F. Stewart, E. R. Davidson, and W. T. Simpson, *J. Chem. Phys.*, **42**, 3175 (1965).
(13) Supplementary material.
(14) B. A. Frenz, J. H. Enemark, and J. A. Ibers, *Inorg. Chem.*, **8**, 1288 (1969).
(15) A. R. Luxmoore and M. R. Truter, *Acta Crystallogr.*, **15**, 1117 (1962).
(16) C. Pedone and A. Sirigie, *Inorg. Chem.*, **7**, 2614 (1968); *Acta Crystallogr.*, **23**, 759 (1967).
(17) F. A. Cotton and P. Lahuerta, *Inorg. Chem.*, **14**, 116 (1975).
(18) H. B. Burgi and J. D. Dunitz, *Helv. Chim. Acta*, **53**, 1747 (1970).
(19) R. G. Little and R. J. Doedens, *Inorg. Chem.*, **13**, 840 (1974).
(20) R. G. Little and R. J. Doedens, *Inorg. Chem.*, **13**, 844 (1974).
(21) C. S. Gibbons and J. Trotter, *J. Chem. Soc. A*, 2659 (1971).
(22) R. Hoxmeier, Ph.D. Dissertation, University of California, Los Angeles, Calif., 1972.
(23) A. P. Krukonis, J. Silverman, and N. F. Yannoni, *Acta Crystallogr., Sect. B*, **28**, 987 (1972).
(24) (a) L. N. Mulay, E. G. Rochow, E. D. Stejskal, and N. E. Weliky, *J. Inorg. Nucl. Chem.*, **16**, 23 (1960); (b) R. K. Bohn and A. Haaland, *J. Organomet. Chem.*, **5**, 470 (1966); (c) see also discussion of this point for the structure of diacetylferrocene, in which an average rotation of 4° 4′ from the eclipsed position is observed for the rings: G. J. Palenik, *Inorg. Chem.*, **9**, 2424 (1970).
(25) L. Pauling, "Nature of the Chemical Bond", Cornell University Press, Ithaca, N.Y., 1960, p 224.

Contribution from the Infrared Spectroscopy Laboratory, University of Bordeaux I, 33405, Talence Cedex, France

Spectroscopic Investigation of Aluminum Trihalide–Tetrahydrofuran Complexes. 1. Structure and Force Fields of the 1:1 and 1:2 Solid Compounds Formed by Aluminum Chloride or Bromide

J. DEROUAULT* and M. T. FOREL

Received December 29, 1976 AIC60926P

The infrared and Raman spectra of AlX_3·THF and AlX_3·2THF (X = Cl or Br) have been recorded. The vibrational analysis is based on the deuterium-isotope effect and on the halogen substitution. The 1:1 compounds have a molecular structure while the 1:2 derivatives correspond to the ionic arrangement $[AlX_2(THF)_4^+, AlX_4^-]$. A complete valence force field has been derived for each 1:1 complex, and a valence force field limited to the AlX_2O_4 part of each 1:2 complex has been estimated. The F(AlO) stretching force constants differ largely between the two types of complex and are consistent with known chemical properties. The main effect of coordination upon the force field is a decrease in the force constant of CO bonds.

Introduction

A structural investigation of coordination compounds formed between aluminum halides and various organic Lewis bases is in progress at the laboratory. The general purpose of this study is to describe the state of coordination of the aluminum atom in donor–acceptor complexes and to provide a way of

identification of intermediate species in catalytic mixtures. The case of tetrahydrofuran (THF) is of great interest since it gives two definite solid derivatives[1] which are stable enough to be analyzed by infrared and Raman spectroscopy.

Previous work on 1:1 adducts, using only the infrared region above 300 cm^{-1}, was published by Lewis et al.[2] We recorded and discussed the infrared spectra above 300 cm^{-1} of the 1:1 and 1:2 adducts,[3,4] but the lack of far-infrared and Raman data made the discussion of the structure difficult and the vibrational assignment uncertain.

We have now recorded the infrared and Raman spectra of the 1:1 and 1:2 adducts between 4000 and 30 cm^{-1} using Cl and Br as the halogen and C_4H_8O and C_4D_8O as a Lewis base. In this paper we discuss the infrared and Raman spectra, basing the assignments on the deuterium-isotope effect, the halogen substitution, and our recent assignment of THF.[5] We also report a complete normal-coordinate analysis for the 1:1 and a simplified normal-mode calculation for the 1:2 adducts.

The former calculation allows the comparison of the force fields of bound and free THF. Furthermore, the assumptions made in the present calculation are identical with those of our previous calculation of $(CH_3)_2O{\cdot}AlX_3$ compounds.[6] This condition makes possible a comparison between the force constants of $O{-}AlX_3$ groups in $(CH_3)_2O$ and in THF adducts. The simplified normal-mode calculation of models for a disubstituted hexacoordinated aluminum atom provides further support for the spectral assignment of 1:2 adducts and for the discussion of their stereochemistry.

Experimental Section

Aluminum chloride and bromide were high grade Fluka products. They were resublimated just before use. Hydrogenated and perdeuterated tetrahydrofurans were spectrograde (Merck). Therefore, we attempted no further purification, but dried the material before use by distillation onto P_2O_5 in vacuo.

The complexes were prepared from a saturated solution of aluminum halide in THF in a conventional vacuum line. The 1:2 adducts were isolated by simple evaporation of the solution, washed with carbon tetrachloride, and dried by condensing the CCl_4 in a nitrogen trap isolated from the pump. Despite these precautions, the recorded Raman spectra of the 1:2 compounds showed an intense fluorescence. This was especially serious for the brominated derivatives, for which only very intense bands could be recorded in the range above 300 cm^{-1}. For purposes of identification, the x-ray diagram powder of $AlCl_3{\cdot}2THF$ was recorded (see Table A[27]).

The 1:1 adducts were prepared from the corresponding 1:2 compounds by pumping at 60 °C under ca. 0.05 Torr for about 1 h. The obtained powders were used directly for infrared analysis. In order to avoid the intense fluorescence in the Raman spectra, the 1:1 samples were distilled in an all-glass apparatus at ca. 140 °C under 0.05 Torr. The stoichiometry of the bis adducts was monitored by weighing the initial amount of $AlCl_3$ (or $AlBr_3$) and by following the weight loss during the evaporation of THF. At last, the final sample was chemically analyzed for its halogen content. The results led to a satisfactory value for the ratio [THF]/[AlX_3] (typically 1.97 ± 0.03). The conversion of the bis adducts into mono adducts was monitored also by weighing, and the halogen content was analyzed in the final sample. The results correspond to the 1:1 stoichiometry within experimental error. The compounds were handled and stored in a drybox. The infrared spectra above 160 cm^{-1} of the Nujol and C_4Cl_6 mulls of these adducts were recorded in CsI cells with a Perkin-Elmer 180, using standard settings (2-cm^{-1} resolution at 2600 cm^{-1}). The range below 250 cm^{-1} was investigated with a RIIC instrument, using a cell mounted with high-density polyethylene windows.

The Raman spectra were recorded from powders stored in on-line sealed glass tubes. The instrument was either a Coderg T 800 triple monochromator or a Coderg Pho double monochromator, using either a 164 or a 165 Spectra-Physics Ar^+ laser, tuned at 488 nm. The spurious lines of the argon plasma were removed with an interferometric filter. The resolution was about 2 cm^{-1} over the total frequency range, and dc amplification mode was used.

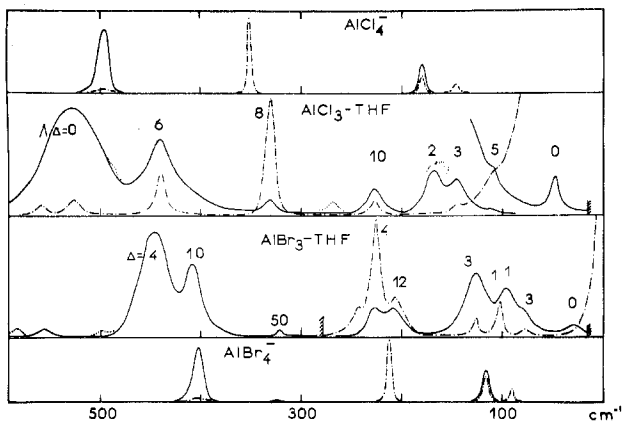

Figure 1. Infrared and Raman spectra below 600 cm^{-1} of hydrogenated $AlX_3{\cdot}THF$ compounds. Solid lines indicate infrared and dashed lines Raman. Isotopic shift $\Delta\nu(H{-}D)$ are written near each band. When the spectrum of d_8 compounds looks different, a dotted line is drawn for it. Λ stands for a weak IR band observed at the nitrogen temperature only.

Infrared and Raman instruments were calibrated using standard references. We found that the accuracy was better than 2 cm^{-1} for all wavenumbers.

The normal-mode calculations were performed on a CII Iris 80 computer, using programs written at the laboratory.[7]

$AlX_3{\cdot}THF$ 1:1 Complexes

Assignment of $O{-}AlX_3$ Groups below 550 cm^{-1}. Figure 1 presents the infrared and Raman spectra of $AlCl_3{\cdot}THF$ and $AlBr_3{\cdot}THF$ below 600 cm^{-1}. Frequency shifts upon deuteration are indicated, and spectra of $AlCl_4^-$ and $AlBr_4^-$ are drawn for comparison. These spectra show that no band of the adducts corresponds to the AlX_4^- anions, while nearly all of them exhibit a shift upon deuteration and upon halogen substitution. This result demonstrates a molecular struture.[8] Furthermore, the spectra fit quite well to the now familiar pattern of monomeric pseudotetrahedral $L{-}AlX_3$ complexes.[10] Earlier structural interpretations[2-4] are thus confirmed, and the assignments are easily made by comparison with analogous equimolecular adducts.[10,11] Because of the possible activity of lattice modes, the assignment of low-frequency bands may be ambiguous. However, all the observed bands for the THF complexes correspond to those of dimethyl ether derivatives.[10] Since the latter had been examined in the form of liquid samples, we conclude that all the spectra of the THF adducts arise from internal modes.

The degenerate stretching mode $\nu_d(AlX_3)$ is observed at 526 and 438 cm^{-1} for the chlorinated and brominated derivatives, respectively. The symmetric stretching mode appears at 328 (X = Cl) and 226 cm^{-1} (X = Br). The XAlX bending modes are observed in the 170–120 cm^{-1} range, while the OAlX bending modes are assigned to the bands below 110 cm^{-1}. The stretching vibration of the coordination bond $\nu(AlO)$ must correspond to the band at 440 cm^{-1}, shifted down at 408 cm^{-1} by Cl/Br substitution. Wagging and twisting motions of the whole ligand with respect of the $O{-}AlX_3$ framework are responsible for the absorption and Raman bands near 200 cm^{-1}, while the $t(AlO)$ torsional vibration appears at 48 (Cl) and 30 cm^{-1} (Br).

Assignment of THF Modes. Since the wavenumbers greater than 50 cm^{-1} are not very sensitive to halogen substitution, we show only one type of complex in the spectra. The figures which are used in the discussion correspond to the frequencies of chlorinated compounds. Figures 2, 3, 4, and 5 show the spectra of the various complexes. The corresponding spectra of free molecules are also shown in order to facilitate the discussion. We do not discuss the assignment of the stretching modes $\nu(CH_2)$ and $\nu(CD_2)$, since the Fermi resonances give

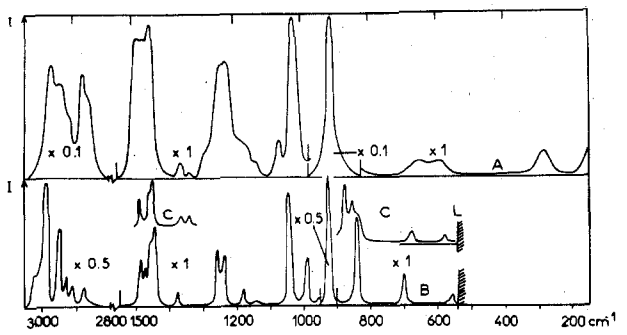

Figure 2. Raman spectra of free and bound THF. Units for scattered intensities are arbitrary. A = liquid THF; B = solid $AlCl_3$·THF; C = limited ranges in which 1:2 compound leads to a different spectrum; $\times R$ = magnication coefficient for intensities; L = below this limit, see Figure 1.

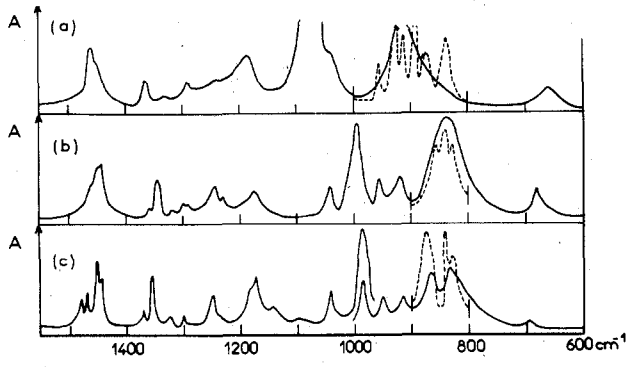

Figure 3. IR spectra of free and bound THF: (a) liquid THF, (b) $AlBr_3$·2THF, (c) $AlBr_3$·THF. The complexes are examined as Nujol and C_4Cl_6 mulls. Dotted line: spectra at liquid nitrogen temperature.

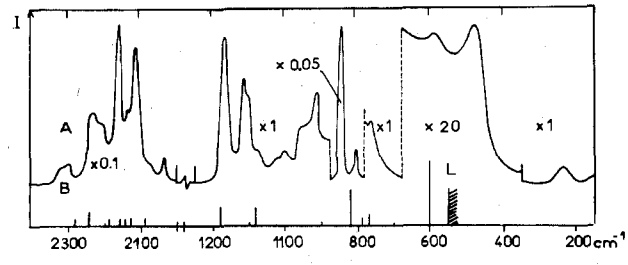

Figure 4. Raman spectra of free and bound THF-d_8: A = liquid C_4D_8O; B = solid $AlBr_3$·C_4D_8O. Owing to an intense fluorescence, only the positions and relative intensities of the peaks are shown. For other symbols see Figure 2.

rise to highly complicated spectra.[5] We note, however, an increase in the frequencies of all maximums and some changes in the relative intensities due to the alteration of the levels involved in the Fermi resonances.

Regarding the hydrogenated derivatives, the formation of the coordination bond leads to weak shifts of THF modes (Figures 2 and 3), and the assignment of free THF may be transferred. We note only the appearance of an overtone or combination infrared band at 1356 or 1326 cm^{-1} since only three wagging modes of the CH_2 groups are expected in this frequency range, and we observed four absorptions (Figure 3). The strongest infrared band is shifted from 1070 to 938 cm^{-1} by the formation of the complex. It is assigned to a ring stretching mode involving the antisymmetric CO stretching (R_1).[12] The Raman intensity at 1042 cm^{-1} may be compared to that observed at 1030 cm^{-1} for the second ring mode (R_2). This mode is not very sensitive to coordination and must therefore involve mainly C–C stretchings. The strongest Raman line must be assigned to the "breathing" ring mode (R_3). It occurs at 924 cm^{-1} (Figure 2) and not at 840 cm^{-1}, as we previously claimed.[3] The mean infrared band at 954

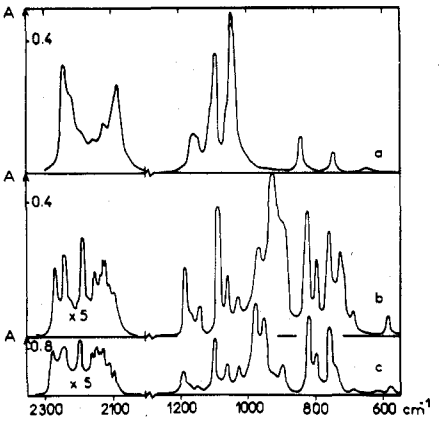

Figure 5. Infrared spectra of free and bound THF-d_8 (A = absorbance): (a) THF-d_8 (thickness 0.02 cm) [below 1025 cm^{-1} solution in CS_2 (c 18 g L^{-1}); above 1025 cm^{-1}, solution in CCl_4 (c 18 g L^{-1})]; (b) $AlBr_3$·THF-d_8 (mull in Nujol); (c) $AlBr_3$·2THF-d_8 (mull in Nujol).

cm^{-1}, which has no Raman counterpart, arises from the rocking mode of methylene groups, which is expected in this range. The wavenumbers and relative intensities of the infrared bands at 863 and 836 cm^{-1} are strongly affected by the conversion of the 1:1 adduct to the 1:2 complex (Figure 3). This demonstrates that the stretching of the CO bonds contributes strongly to these vibrations. Therefore, we assign these bands to the ring modes R_4 and R_5. The ring bending mode, which involves mainly the COC angle (R_6), is shifted from 655 cm^{-1} for free THF to 698 cm^{-1} for the complexes. The ring bending modes R_7 and R_8 are observed at 566 (Figure 2) and 322 cm^{-1} (Figure 1), respectively.

Figures 4 and 5 show that the infrared and Raman spectra of THF-d_8 are deeply modified by the formation of the 1:1 adducts. However, some points may be outlined. In Figure 5, we see a shift of the infrared intensity toward modes with lower wavenumbers; this is indicative of a weakening of CO bonds. Thus, only one intense infrared band stays between 1040 and 1200 cm^{-1}, while a strong and broad feature is observed near 920 cm^{-1}; it arises from one or several modes involving ν_a(COC). Among the bending and rocking CD_2 modes, those which appeared above 950 cm^{-1} for free THF-d_8[5] are slightly affected by coordination. The strongest Raman line at 826 cm^{-1} must be assigned to the ring breathing mode. The weak infrared bands at 586 (Figure 5) and 270 cm^{-1} (Figure 1) correspond to the R_6 and R_8 modes. On the infrared spectrum of $AlBr_3$·THF-d_8, the weak shoulder at 485 cm^{-1} may correspond to the R_7 mode. The assignment of other bands can only be made with the use of a normal mode calculation. No band may be assigned to the pseudorotation mode of THF or THF-d_8.

Normal-Coordinate Analysis. The normal modes of the complex molecules have been calculated using the **GF** matrix method[13] on the basis of a valence force field. We have assumed that the geometry of the THF molecule does not change upon complexation and have chosen the structure previously described for the O–AlX_3 moiety;[6] the COAl angles were assumed initially to be equal to 109° 28′. The coordinates and the geometrical parameters (Table B[27]) were consequently taken from those of THF[5,14] and those of the (C_2) O–AlX_3 framework.[6] The first calculation was made with an **F** matrix, which was essentially composed by the sum of the recently determined force field of free THF[5] and of the force field corresponding to the framework of analogous dimethyl ether adducts.[6] Some additional force constants, related to interactions between the two moieties, have also been introduced. The potential-energy distribution obtained through this first calculation shows a fairly good agreement with the assignment,

Table I. Force Field of Free and Bound Tetrahydrofuran[a]

Diagonal Constants			Off-Diagonal Constants[b]					
Coordinate	F, free	F, bound	Coordinates	f, free	f, bound	Coordinates	f, free	f, bound
ν_a	4.77	4.81[d]	δ_i, w_{i+1}*	0.048	0.043	r_i, α_{i+1}	0.024	0.017
ν_s	4.59	4.64[d]	δ_i, R_i	−0.092	0.038	D, D	0.467	0.526
δ_1	0.518	0.523	δ_i, α_i	−0.009	0.076	R_i, R_{i+1}	0.302	0.270
δ_2	0.495	0.483	δ_i, α_{i+1}	0.036	0.092	D_1, R_2; R_4, D_5	0.302	0.400
w	0.733	0.761	w_i, w_{i+1}	−0.067	−0.073	R_i, α_i	0.502	0.502
t	0.650	0.645	w_i, w_{i+2}	−0.004	−0.005	D, β	0.557	0.536
r	0.676	0.691	w_i, R_i*	−0.279	−0.302	α_i, α_{i+1}	0.193	0.201
D	4.41	3.50	w_2, D_1[c]	−0.264	−0.282	α_i, α_{i+2}	0.123	0.120
R	4.44	4.44	t_i, t_{i+1}	0.030	0.037	α_i, τ_i[f]	0.036	0.036
α	1.28	1.23	t_i, t_{i+2}	−0.032	−0.035	τ_i, τ_{i+1}[e,f]	0.009	0.009
β	1.40	1.48	r_i, r_{i+1}	−0.021	0.019	τ_i, τ_{i+2}[f]*	−0.007	−0.007
τ	0.087	0.131	r_i, r_{i+2}	−0.009	0.062	β, AlO		−0.007
D_1, r_2; D_5, r_5		0.068	r_i, t_{i+1}*	−0.041	−0.042	β, ν_S		−0.161

[a] Units of force constants are: mdyn A^{-1} for bonds, mdyn A rad^{-2} for angles, and mdyn rad^{-1} for bond angle interactions. Notations for local symmetry coordinates are: $\delta_1 = CH_2$ scissoring, α position from O; $\delta_2 = CH_2$ scissoring, β position from O; w = CH_2 wagging; t = CH_2 twisting; r = CH_2 rocking; R = CC stretching; D = CO stretching; α = CCC or OCC bending; β = COC bending; τ = torsions with respect of CC bonds; ν_a = antisymmetric CH_2 stretching; ν_S = symmetric CH_2 stretching; AlO = AlO stretching; and ν_S = symmetric AlX_3 stretching. For definitions of local coordinates, see ref 18. Subscripts i refer to diagram A in table B[27] for the coordinates δ, w, t, r, and α and to diagram B in Table B[27] for the coordinates R, D, and τ. [b] When CC and CO bonds (or CCC, CCO and COC angles) have not been distinguished, we only write R (or α). When coordinates are oriented in space, the sign of related interaction force constants depends on the writing of these coordinates. With nonoriented coordinates, we have: $f(a_i, b_{i+1}) = f(a_i, b_{i-1})$; with oriented angular coordinates, we have: $f(c_i, d_{i+1}) = -f(c_i, d_{i-1})$. In case of torsional motions, we have $f(\tau_i, \tau_{i+1}) = f(\tau_i, \tau_{i-1})$ and $f(\tau_i, \tau_{i+2}) = -f(\tau_i, \tau_{i-2})$. Only the figures relative to the left members of these relations are listed; asterisks indicate when the sign may change. [c] $f(w_5, D_5) = -f(w_2, D_1)$. [d] For the $AlBr_3$-THF adduct, slightly lower experimental wavenumbers for $\nu(CH_2)$ modes lead to $F(\nu_a) = 4.77$ and $F(\nu_s) = 4.62$. [e] This force constant was transferred from the cyclohexane force field.[18] It was only corrected for the number of dihedral angles related to the motion. We attempted no further adjustments for THF. [f] These force constants have not been adjusted in the calculation of complexes.

but important discrepancies exist between experimental and calculated wavenumbers, even when the F[CO] force constant is lowered.

At this stage, we had to choose an approach in order to improve the results. We used the program written at the laboratory,[7] which is based on an iterative method.[15-17] In such complicated systems, the force constants are not indepenent and are correlated together through a number of relations. Our program allows the determination of these relations, assuming the eigenvectors are submitted to weak alterations. Subsequently, when one force constant is adjusted, the modifications of all correlated force constants are taken into account.[17] The lack of isotopic derivatives of $AlCl_3$ or $AlBr_3$ and the sensitivity of the results on the value of the COAl angle prevent us from achieving a genuine refinement. Therefore, we have adjusted only some significant force constants, applying the modifications of the other force constants as outlined above. Nevertheless, these later force constants are only slightly modified with respect to their value in the initial calculation. Concerning the THF part, a better agreement is obtained by an increase of the stretching force constants $F[\nu(CH_2)]$ which approximately accounts for the increase of wavenumbers, an important decrease of the force constant $F[\nu(CO)]$, and the behavior of the interaction $f[\nu(CO), r\text{-}(CH_2)_\alpha]$. We have also made some attempts to adjust some force constants of the O–AlX_3 groups; however, the isotopic effect of deuteration was not conveniently transferred from the THF to the O–AlX_3 framework, whatever the force field. The only way to improve the accuracy of calculated isotopic shifts was to increase the value of the COAl angles. A good agreement with experimental data was obtained when the value of the angle reached 120°.

The force fields are listed in Tables I and II, and Tables III and IV present the comparison between experimental and calculated frequencies.

It is of interest to compare the data related to the O–AlX_3 groups of $(CH_3)_2O$ and THF addition compounds. For the $(CH_3)_2O$ adducts,[6] examination of the eigenvector matrices has shown a very low degree of vibrational mixing between the O–AlX_3 groups and the organic ligand. We now have the reverse situation since numerous internal coordinates of THF contribute appreciably to the normal modes which mainly refer to the O–AlX_3 vibrations. This latter property explains the possibility of accounting for the H/D substitution effect by changing the value of the COAl angle. Furthermore, the stretching of the AlO bond contributes to several normal modes, of which some arise mainly from internal THF motions. With respect to the force fields, the numerical values of the O–AlX_3 force constants depend only slightly on the Lewis base. It is significant, nevertheless, to note the increase of the coordination bond force constant and the slight decrease of the average value of the force constants in the three AlCl bonds when $(CH_3)_2O$ is replaced by THF. The same result is obtained with $AlBr_3$ adducts. These remarks are quite consistent with the fact that the complexes with THF are chemically stronger, despite the observation that the frequencies of bands mainly corresponding to ν(AlO) are much lower.

Table II. Valence Force Field of the O–AlX_3 Groups in AlX_3·THF 1:1 Adducts[a]

	F_{ii}			f_{ij}	
	X = Cl	X = Br		X = Cl	X = Br
AlO	2.14	2.14	AlO, $\nu_s(AlX_3)$	0.07	0.28
AlX_s	2.34	2.20	AlX, AlX	0.13	0.16
AlX_a	2.24	1.98	$\nu_s(AlX_3)$, $\delta_s(AlX_3)$	0.22	0.21
$\delta_s(AlX_3)$	0.57	0.74	AlO, $\delta_s(AlX_3)$	−0.43	−0.36
$\delta_s'(AlX_3)$	0.62	0.87	$\nu_s'(AlX_3)$, $\delta_s'(AlX_3)$	−0.23	−0.30
$\delta_a(AlX_3)$	0.67	0.87	$\nu_a(AlX_3)$, $\delta_a(AlX_3)$	−0.25	−0.29
$r_{\|\|}(AlX_3)$	0.90	0.72	$\delta_s'(AlX_3)$, $r_{\|\|}(AlX_3)$	0.08	0.15
$r_\perp(AlX_3)$	0.89	0.60	$\delta_a(AlX_3)$, $r_\perp(AlX_3)$	0.03	0.12
τ(AlO)	0.1	0.05	$\nu_s'(AlX_3)$, $r_{\|\|}(AlX_3)$	0.25	0.28
w(THF)	0.51	0.49	$\nu_a(AlX_3)$, $r_\perp(AlX_3)$	0.24	0.28
t(THF)	0.46	0.51	w(THF), $r_{\|\|}(AlX_3)$	0.13	0.13
			t(THF), $r_\perp(AlX_3)$	−0.13	−0.09
			w(THF), $\nu_s(AlX_3)$	0.34	0.28
			δ(COC), $\nu_s(AlX_3)$	−0.16	−0.16
			δ(COC), ν(AlO)	−0.007	−0.001

[a] Units and notation: see Table I and ref 6.

Table III. Low Frequencies of the $AlX_3 \cdot THF$ 1:1 Adducts[a]

$AlCl_3$					$AlBr_3$			
ν_{expt}, cm^{-1}		ν_{calcd}, cm^{-1}		Assignments	ν_{expt}, cm^{-1}		ν_{calcd}, cm^{-1}	
THF	$\Delta\nu$(H-D)	THF	$\Delta\nu$(H-D)		THF	$\Delta\nu$(H-D)	THF	$\Delta\nu$(H-D)
525	0	522	0	$\nu_s'(AlX_3)$	438	4	437	2
		520	0	$\nu_a(AlX_3)$			428	0
439	6	436	10	ν(AlO)	408	10	407	14
330	8	326	6	$\nu_s(AlX_3)$	224	4	231	2
228	10	234	9	w (THF)	206	12	212	14
		226	10	t (THF)			201	15
167	2	171	1	$\delta_s'(AlX_3)$	125	3	125	1
159[c]	...	167	2	$\delta_a(AlX_3)$			123	1
145	3	146	3	$\delta_s(AlX_3)$	103	1	111	3
109	5	129[b]	11	$r_{\|\|}(AlX_3)$	95	1	104	10
		115	7	$r_\perp(AlX_3)$	78	3	75	4
48	0	47	4	τ(AlO)	31	0	31	3

[a] The experimental wavenumbers are the average values from the infrared and Raman data. The assignments refer to the main coordinate of each normal mode. [b] The calculated splitting between $r_{||}$ and $r_\perp$ modes is anomalously large because of an interaction with the highly anharmonic pseudorotational mode.[5] [c] Wavenumber of the deuterated compound.

Table IV. Wavenumbers and Modes of Bound THF and THF-d_8[c]

C_4H_8O				C_4D_8O			
Free[a]	Bound ($AlCl_3$–C_4H_8O)			Free[b]	Bound ($AlCl_3$–C_4D_8O)		
ν_{exptl}	ν_{exptl}	ν_{calcd}	Mode	ν_{exptl}	ν_{exptl}	ν_{calcd}	Mode
1487	1482	1477	δ_1, w, δ_2	1165	1187	1177	R, w, δ_1, β
1478	1470	1470	δ_2, w	1150	1165	1139	w, R
1458	1453	1459	δ_2, δ_1, w		1144	1137	R, δ_1, δ_2, w
1444	1448	1445	δ_1, δ_2	1109		1136	w, R, δ_2
1365	1372	1377	w, R	1098 (IR)	1086	1094	δ_2, δ_1, α
1332	1326	1337	w	1073		1069	δ_2, δ_1, R, w
1288	1302	1295	w, R	1060 (IR)	1060	1063	δ_1, δ_2, w, R
1240	1251	1263	w, t, δ_1	1044 (IR)	1033	1021	w, δ_1, A
1230 (R)	1236	1234	t, w	951	968	960	r
1185	1186	1186	t	922	925	909	t, D
1175 (R)	1176	1175	t		910	881	D, w, t
1140 (R)	1144	1144	r			864	A, t, w
		1062	t			853	t, w, R
1070	988	997	R, r, A, α			838	t
1030	1042	1048	R, t, α	842		819	t, r, R
956	954	947	r, R	800	826 (R)	803	t, R, S, r
918	924 (R)	936	R	760	798	767	R, w, t
909	912	911	R, r, α	746 (IR)	768	752	r, R, t, w
888	890	880	S, R, r			728	t, r
870	863	851	A, r, α	706 (S)		710	r, t, A, α
840	836	826	r, D	641	692	669	r, S, α
655	698	697	α, S, β	580	586	611	r, α
581	566	572	α	471	485	501	α, r
286	322	310	τ, α	235	270	250	τ, α

[a] Experimental wavenumbers are those of the IR spectra, but some are observed only on the Raman spectrum. The latter are noted (R). [b] Experimental wavenumbers are those of the Raman spectrum, but some are observed only on the infrared spectrum of solutions (IR) or of the solid (S). [c] The form of normal modes is suggested from the potential energy distribution. It is calculated according to the formula PED = $100L_{ik}{}^2F_{ii}/\lambda_k$ in which λ_k stands for the frequency parameter, F_{ii} the force constant, and L_{ik} the eigen vector. Abbreviations are those of Table I, with the addition: A = combination of D similar to ν_a(COC); S = combination of D similar to ν_s(COC).

Among the modes of C_4H_8O (Table VI), the motions of methylene groups above 940 cm^{-1} are very slightly sensitive to the coordination. The modes at 1042, 924, and 566 cm^{-1} involve essentially the CC stretchings and CCC and OCC bendings, as in the case of free THF. The contribution of CO bonds in the ring mode at 698 cm^{-1} becomes important. In free THF, the ν_a(COC) vibration contributes to the modes at 1070 and 909 cm^{-1}, but mainly to the former.[5] For the adducts, ν_a(COC) is again involved in the two modes at 988 and 863 cm^{-1}, but the main contribution occurs at the lower frequency. This is consistent with the change of relative intensities which is observed on the infrared spectra (Figure 3).

Regarding the modes of C_4D_8O (Table VI), most of them are affected by the formation of the adduct. For these adducts, the potential energy related to CO stretching participates in the modes at lower frequency. This is consistent with the previously discussed changes in the intensities. The COC bending does not contribute significantly in ring modes, but participates in several O–AlX_3 modes.

Concerning the force field of THF, the force constant of CC bonds remains unaffected, and those of methylene groups are slightly sensitive to the coordination. According to the Siebert formula,[19] the final value obtained for the CO force constant, 2.14 mdyn $Å^{-1}$, corresponds to a bond order close to 0.65. This result may be compared to the ability of THF to undergo a ring opening and to polymerize in the presence of certain Lewis acids.[20]

$AlX_3 \cdot 2THF$ 1:2 Complexes

Vibrational Spectra and Assignment. Nearly all of the spectral features which correspond to bound THF and THF-d_8

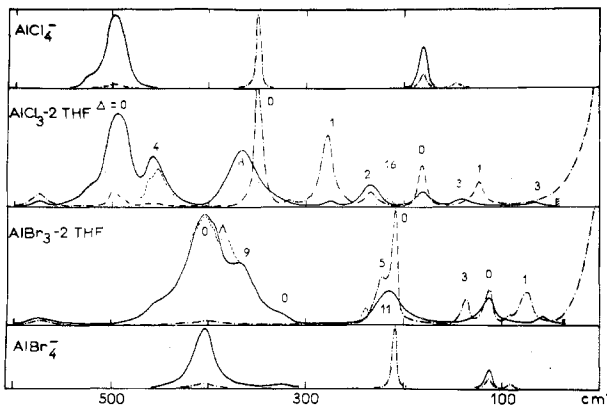

Figure 6. Infrared and Raman spectra below 600 cm^{-1} of hydrogenated $AlX_3 \cdot 2THF$ compounds. Legend: see Figure 1.

are slightly sensitive to the coordination number (Figures 2–5). Therefore the assignment of 1:1 adducts may be kept. The main differences concern the modes involving the CO bonds (near 1000 and 850 cm^{-1}). The decrease of frequencies with respect to the free molecules is lower in the case of 1:2 adducts. This fact is consistent with the results obtained for the $(CH_3)_2O$ adducts,[21] in which the effect of coordination upon the ligands decreases when the coordination number increases. Figure 6 shows the infrared and Raman spectra of $AlCl_3 \cdot 2THF$ and $AlBr_3 \cdot 2THF$ below 600 cm^{-1}. Frequency shifts upon deuteration are indicated, and the spectra of $AlCl_4^-$ and $AlBr_4^-$ are also drawn for comparison. This permits easy identification of the characteristic bands of the $AlCl_4^-$ and $AlBr_4^-$ anions in the spectra of the chlorinated and brominated complexes. This assignment is supported by the zero isotopic shifts upon H/D substitution of these bands. The second piece of evidence is the presence of several bands which are shifted upon Cl/Br substitution and which do not belong to the AlX_4^- spectra. This demonstrates that in the cations some halogen atoms are bound to the aluminum.

Among the numerous possible formulas corresponding to the 1:2 stoichiometry, only the ionic arrangement $[AlX_4^-, AlX_2(THF)_4^+]$ is consistent with the above conclusions. This cation probably represents the first instance where such a mixed octahedron is identified in solid-state aluminum chemistry. A similar ionic complex, $[FeCl_2(DMSO)_4^+, FeCl_4^-]$, is known among the iron(III) derivatives.[22]

The final open question arising in our structural discussion of the spectra is the configuration of the octahedral cation. In the case of a trans configuration, the symmetry type would correspond to the D_{4h} point group if we consider the THF ligand as a single atom. The irreducible representation of the AlX_2O_4 framework is shown in eq 1, where g modes are

$$\Gamma = 2A_{1g} + 1B_{1g} + 1B_{2g} + 1E_g + 2A_{2u} + 1B_{2u} + 3E_u \quad (1)$$

Raman active and u modes, except for the B_{2u} type, are infrared active. Under the same assumptions, the cis form has C_{2v} symmetry; this leads to the irreducible representation shown in eq 2, where all modes are infrared and Raman active,

$$\Gamma = 6A_1 + 2A_2 + 4B_1 + 3B_2 \quad (2)$$

except for the A_2 modes which are infrared forbidden. Nevertheless, these selection rules may relax since the actual symmetry type is probably lower than the above considered cases owing to the geometry and relative position of THF ligands and the packing inside the primitive unit cell of the lattice.

Some features of the spectra have to be discussed before we can choose between these configurations. For the chlorinated compounds, we note the very weak isotopic shift of the Raman line at 284 cm^{-1}. We also note that the isotopic shifts of the bands near 230 cm^{-1} are different in the infrared (2 cm^{-1}) and the Raman (16 cm^{-1}). Consequently, we conclude that these bands do not belong to the same mode. A problem arises concerning the weak Raman line at 318 cm^{-1}; it was definitely observed only for the $AlCl_3 \cdot 2C_4H_8O$ compound. We believe that this band may correspond to a THF mode as well as to a $AlCl_2O_4$ framework vibration.

The infrared spectrum of $AlBr_3 \cdot 2C_4H_8O$ shows a shoulder near 440 cm^{-1}; its intensity varies from sample to sample, and must therefore correspond to the most intense absorption of a small amount of a 1:1 complex impurity (Table III). A strong infrared band is observed at 382 cm^{-1} for $AlBr_3 \cdot 2C_4D_8O$. The corresponding band of the hydrogenated compound must be masked by the prominent $AlBr_4^-$ absorption; the spectrum recorded at the liquid nitrogen temperature effectively reveals a band near 385 cm^{-1}. As in the case of $AlCl_3$ complexes, the infrared and Raman bands near 220 cm^{-1} do not correspond to the same mode, as judged by their different isotopic shifts.

The mutual exclusion between infrared and Raman active modes therefore appears nearly perfect for both complexes. This property and the number of observed bands fit fairly well the required conditions for the trans configuration of the cation. According to this assumption, the spectra may now be assigned as follows: (1) $\nu_d(AlO_4)$ (E_u) is always observed at about 360 cm^{-1}. (2) $\nu_a(AlX_2)$ (A_{2u}) shifts from 460 to 380 cm^{-1} upon Cl/Br substitution. The shoulder observed for $AlCl_3 \cdot 2C_4D_8O$ arises probably from either crystal effects or a bending mode of the THF rings. (3) For the chlorinated compounds, the stretching A_{1g} modes $\nu_s(AlCl_2)$ and $\nu_s(AlO_4)$ are observed at ca. 280 and 230 cm^{-1}, respectively. (4) For the brominated complexes, the stretching vibrations $\nu_s(AlO_4)$ and $\nu_s(AlBr_2)$ suffer probably a strong coupling since they are both expected in the same narrow range. The resulting A_{1g} modes are observed at 220 and 137 cm^{-1}. (5) The remaining stretching vibration, $\nu_s'(AlO_4)$ (B_{1g}), may be expected between the positions of the $\nu(AlO_4)E_u$ and A_{1g} modes by comparison with analogous entities.[23,24] The Raman band observed for $AlCl_3 \cdot 2C_4H_8O$ near 320 cm^{-1} must correspond to this $\nu_s'(AlO_4)$ vibration, unless, as we have discussed above, it is due to a THF mode. (6) The same comparison[23,24] leads to an assignment of the other bands in the 200 and 100 cm^{-1} ranges to the OAlO and OAlX bending modes if we suppose that lattice modes are not observed. Since lattice modes were not observed for the 1:1 compounds, we feel that this assumption is reasonable. (7) The weak bands at about 570 cm^{-1} for all the compounds and the weak infrared band at 240 cm^{-1} for $AlBr_3 \cdot 2C_4D_8O$ (Figure 2) are assigned to various deformation modes of the THF rings.

Normal-Coordinate Analysis of the AlX_2O_4 Model. In order to support the above structural discussion and vibrational assignment of 1:2 complexes, we have performed a simplified normal-coordinate analysis of the AlX_2O_4 cis and trans models, using the Wilson method.[13] The calculation has been limited to such octahedral models because of our ignorance of the relative positions of the THF ligands. The bond lengths used in the above calculation of 1:1 compounds have been transferred to these models, and all angles were taken equal to 90°. The complete set of internal coordinates was used, and the three redundancies were numerically removed during the diagonalization of the **G** matrix.

We had to take into account the interactions of the internal motions of THF with the framework vibrations since they were demonstrated to be important in the above calculation of the 1:1 compounds. The general approach in choosing an appropriate "effective mass" for the oxygen atom was not feasible since we could not estimate this mass by any accurate means. We therefore kept the oxygen mass equal to 16 and determined

Table V. Valence Force Field of the AlX_2O_4 Models[a]

Force constant	X = Cl	X = Br
F(AlO)	1	1
F(AlX)	1.62	1.53
f(AlO, AlO)	−0.10	−0.144
f(AlX, AlX)	0.05	0.1
f(AlX, AlO)	0.02	0.14
F(XAlO)	0.20	0.18
F(OAlO)	0.55	0.51
f(r, α)	0.10	0.10
f'(r, α)	−0.07	−0.07

[a] The units are the same as in Table I. f(r, α) is used when the bond r is along one of the straight lines subtended by the angle α. f'(r, α) is used when the bond r is coplanar with the plane of the angle α with only one common atom.

a set of corrected frequencies, in which the influence of coupling with the ligand is eliminated. For this purpose we have calculated the frequencies of an isolated O–AlX_3 model by using the force field determined for 1:1 adducts. The principal result of this calculation is an increase of the ν(AlO) stretching frequencies of about 130 cm^{-1}. Therefore, the estimated ν(AlO) frequencies of the octahedral model will be considered satisfactory if they are greater than the observed values by about 100 cm^{-1}. The H/D isotope effect has been simulated by changing the oxygen mass by some units.

The force constants have been chosen in order to obtain credible frequencies for both cis and trans models; they are listed in Table V. Under these conditions, the 15 frequencies of the cis model are all modified by the "deuteration" and by the Cl/Br substitution. The potential-energy distributions show that these properties result from the exceedingly complex form of the normal modes to which every internal coordinate contributes.

The trans model leads to normal modes in which the different coordinates appear to be coupled less strongly. On the other hand, the $\nu_a(AlCl_2)$, $\nu_a(AlBr_2)$, and $\nu_s(AlCl_2)$ stretching modes are nearly unaffected by the deuteration and the $\nu_d(AlO_4)$ vibration is only slightly sensitive to the halogen substitution. This result agrees with the experimental data. This last model gives, furthermore, a good description of the coupling which is observed in the Raman spectra between $\nu_s(AlBr_2)$ and $\nu_s(AlO_4)$.

The calculation for the trans hypothesis gives, therefore, the best fit with experimental data and supports the above discussion of the structure. The results are summarized in Table VI.

Some comments can be made about the force constants despite the limitation of the calculation method. The f(AlO–AlO) interaction force constant seems to have a negative value; this is unusual enough and would mean that an increase of one AlO bond length induces an increase of the three others in order to minimize the potential energy of the system.[25] The second point is the very low value of the F(AlO) force constant, about one-half of that obtained for 1:1 complexes. These remarks are consistent with the ability of the 1:2 complexes to undergo easily important modifications of their structure[26] and the easy removal of the second THF molecule to give the 1:1 complexes.

Conclusion

The vibrational spectra of AlX_3·THF and AlX_3·2THF complexes may be quite satisfactorily explained in terms of a molecular structure for the former compounds and an ionic arrangement $[AlX_4^-, AlX_2(THF)_4^+]$ for the latter. The calculated normal modes and frequencies agree with the spectra, and the values of the force constants account for the difference of stability. However, reaction 3, which occurs even

$$[AlX_2(THF)_4^+, AlX_4^-] \rightarrow 2AlX_3 \cdot THF + 2THF \quad (3)$$

Table VI. Assignments and Calculations of the D_{4h} Models AlX_2O_4

	$AlCl_2(THF)_4^+$		$AlBr_2(THF)_4^+$	
D_{4h} modes	ν_{exptl},[d] cm^{-1}	ν_{calcd}, cm^{-1}	ν_{exptl},[d] cm^{-1}	ν_{calcd}, cm^{-1}
$\nu_d(AlO_4)$ E_u	367 (IR)	445[b]	364 (IR)	457[b]
$\nu_a(AlX_2)$ A_{2u}	457 (IR)	456	382 (IR)	380
$\nu_s'(AlO_4)$ B_{1g}	318[a] (R)	342[b]		348[b]
$\nu_s(AlO_4)$ A_{1g}	233 (R)	268[b]	221 (R)	264[b]
δ(OAlO) B_{2g}		254		244
δ(OAlO) E_u	232 (IR)	226	215 (IR)	216
$\nu_s(AlX_2)$ A_{1g}	284 (R)	287	137 (R)	158
δ(OAlX) E_g	127 (R)	127	76 (R)	109
δ(OAlX) A_{2u}	140 (IR)	127		107
δ(OAlX) B_{2u}	c	108	c	103
δ(OAlX) E_u	65 (IR)	79	58 (IR)	55

[a] See text. [b] $\nu(AlO_4)$ wavenumbers are calculated to be greater than experimental values (see text). [c] Forbidden. [d] IR: infrared active; R: Raman active.

at room temperature in the solid phase in vacuo, implies the possibility of ligand migrations in the lattice. The knowledge of the crystal packing would perhaps explain this property.

Acknowledgment. The authors are indebted to Professor Lascombe of the University of Bordeaux for helpful discussions and to Professor P. Granger of the University of Rouen for the ^{27}Al NMR measurement. We also thank Dr. P. Caillet of the University of Rennes for the x-ray measurement and P. Maraval for writing the efficient computer programs.

Registry No. $AlCl_3$·THF, 15283-71-3; $AlBr_3$·THF, 15283-67-7; $AlCl_3$·2THF, 64200-55-1; $AlBr_3$·2THF, 64200-51-7; $AlCl_3$·THF-d_8, 64200-49-3; $AlBr_3$·THF-d_8, 64200-48-2; $AlCl_3$·2THF-d_8, 64200-47-1; $AlBr_3$·2THF-d_8, 64200-45-9.

Supplementary Material Available: Tables A (x-ray powder data for $AlCl_3$·2THF) and B (geometrical parameters for AlX_3·THF) (2 pages). Ordering information is given on any current masthead page.

References and Notes

(1) R. L. Richards and A. Thompson, *J. Chem. Soc. A*, 1244 (1967).
(2) J. Lewis, J. R. Miller, R. L. Richards, and A. Thompson, *J. Chem. Soc.*, 5850 (1965).
(3) M. T. Forel, J. Derouault, J. Le Calve, and M. Rey-Lafon, *J. Chim. Phys. Phys.-Chim. Biol.*, **66**, 1232 (1969).
(4) J. Le Calve, J. Derouault, M. T. Forel, and J. Lascombe, *C. R. Hebd. Seances Acad. Sci., Ser. B*, **264**, 611 (1967).
(5) J. Derouault and M. T. Forel, *Can. Spectrosc.*, to be published.
(6) J. Derouault, M. Fouassier, and M. T. Forel, *J. Mol. Struct.*, **11**, 423 (1972).
(7) M. T. Forel and P. Maraval, to be published.
(8) We have examined the ^{27}Al NMR spectrum of the molten $AlCl_3$·THF adduct. It consists of a unique band located at −98 ppm downfield from $Al(H_2O)_6^{3+}$ as an external reference. This result agrees quite well with the previously found value for the $(C_2H_5)_2O$–$AlCl_3$ adduct[9] and suggests a tetrahedral structure for the liquid complex.
(9) R. G. Kidd and D. R. Truax, *Can. Spectrosc.*, **14**, 1 (1969).
(10) J. Derouault and M. T. Forel, *Ann. Chim. (Paris)*, **6**, 131 (1971).
(11) I. R. Beattie and G. A. Ozin, *J. Chem. Soc. A*, 2373 (1968).
(12) The notation R_i corresponds to the description of ring modes in ref 3.
(13) E. B. Wilson, J. C. Decius, and P. C. Cross, "Molecular Vibrations", McGraw-Hill, New York, N.Y., 1955.
(14) H. M. Seip, *Acta Chem. Scand.*, **23**, 2741 (1969).
(15) J. Shimanouchi and I. Suzuki, *J. Chem. Phys.*, **30**, 296 (1965).
(16) J. H. Schachtschneider and R. G. Snyder, *Spectrochim. Acta*, **19**, 117 (1963).
(17) M. Tranquille, Thesis, University of Bordeaux, 1975, CNRS AO 5315.
(18) M. T. Forel and C. Garrigou-Lagrange, *Ann. Chim. (Paris)*, **8**, 207 (1973).
(19) H. Siebert, *Z. Anorg. Allg. Chem.*, **273**, 170 (1953).
(20) G. A. Olah, "Friedel-Crafts Chemistry", Wiley-Interscience, New York, N.Y., 1973.
(21) J. Derouault, Thesis University of Bordeaux, 1968.
(22) M. J. Bennett, F. A. Cotton, and D. L. Weaver, *Acta Crystallogr.*, **23**, 581 (1967).
(23) K. Nakamoto, "Infrared Spectra of Inorganic and Coordination Compounds", 2nd ed, Wiley-Interscience, New York, N.Y., 1970.
(24) D. W. James and M. J. Nolan, *J. Raman Spectrosc.*, **1**, 271 (1973).
(25) L. H. Jones, *Coord. Chem. Rev.*, **1**, 351 (1966).
(26) J. Derouault, P. Granger, and M. T. Forel, *Inorg. Chem.*, following paper in this issue.
(27) Supplementary material.